

## CONSEQUENCES OF INTERNAL STRESSES GENERATED BY HYDRATION ON THE CONCRETE MECHANICAL BEHAVIOUR

M. BRIFFAUT<sup>\*</sup>, F. BENBOUDJEMA<sup>\*\*</sup>, C. LABORDERIE<sup>†</sup> AND J.M. TORRENTI<sup>††</sup>

<sup>\*</sup> University Joseph Fourier-Grenoble I, Grenoble-INP, CNRS UMR 5521  
Laboratoire 3S-R, Domaine Universitaire, BP53, 38041 Grenoble Cedex 9, France,  
Email : briffaut@geo.hmg.inp.fr

<sup>\*\*</sup> LMT-Cachan, ENS-Cachan, Paris 6 University, CNRS, UniverSud Paris PRES, France

<sup>†</sup> SIAME EA-4581 Université de Pau, France

<sup>††</sup> Université Paris-Est, IFSTTAR, France

**Key words:** Durability concrete hydration, basic creep, mesoscopic simulation, micro-cracking

**Abstract:** At early-age, hydration of cement leads to a reduction of volume (caused by the Le Chatelier contraction) which induces autogeneous shrinkage. Besides, hydration is an exothermic reaction and an increase of temperature occurs (followed by a decrease). As autogeneous shrinkage arises only in cement paste and as coefficient of thermal expansion may be different between cement paste and aggregates, strains incompatibilities lead to an internal self-equilibrated state of stress. Depending especially on the concrete mix, initial cracking may occur at the cement paste scale leading to a modification of the global concrete behavior.

In this contribution, an analysis of the internal stresses is performed on a mesoscopic mesh by finite element calculations taking into account hydration, autogeneous and thermal shrinkage, basic creep and cracking.

Influence of creep strains and mesoscopic representation are studied showing that, for an ordinary concrete, hydration lead to a reduction of “elastic” stiffness and tensile strength even if creep is taken into account.

### 1 INTRODUCTION

At early-age, hydration of cement leads to a reduction of volume (Le Chatelier contraction) which induces autogeneous shrinkage. Moreover, hydration is an exothermic reaction: an increase of temperature is followed by a decrease. If endogenous and thermal strains are restrained, compressive stresses and then tensile stresses rise, which can reach the concrete strength and thus lead to crossing cracks. Besides, autogeneous shrinkage occurs only in cement paste and coefficient of expansion may be different between cement paste and aggregates. These strains incompatibilities lead to an internal self-

equilibrated state of stress: tensile stresses in cement paste and compressive ones in aggregates are generated. Therefore, initial cracking may occur in the cement paste, depending especially on the concrete mix. Indeed, when the water to cement ratio decreases and cement content increases (for High Performance Concrete for example), the autogeneous shrinkage and the global hydration heat (and associated elevation of temperature) increase and enhance the risk of cracking. It is similar to the case of drying or at elevated temperature: drying shrinkage of cement paste is restrained by aggregates, therefore cracking may occur in the cement paste. The case of drying shrinkage

incompatibilities has been studied in several studies at ambient temperature [1-6] or at elevated temperatures [7-10], but it is not the case of autogeneous and thermal shrinkage at early age [11].

In this contribution, an analysis of the internal stresses will be performed at early age on a Representative Elementary Volume (REV) of concrete considering two phases: cement paste and aggregates. Internal transition zone (ITZ) which thickness around aggregate increases as the w/c ratio decreases [12] is not taken into account explicitly. The assumed properties of cement paste are an average of the ones of cement paste and ITZ. Finite element calculations using Cast3m are undertaken with the taking into account (in the cement paste) of hydration, autogeneous and thermal shrinkage, basic creep [13] and cracking (damage and plastic-damage model which could including the computation of crack opening [14-15]). Drying and associated drying shrinkage are not considered here due to the fact that this study concerns only massive concrete structures at early-age (drying is a very slow process affecting at early age only a few centimeters depth of concrete [16]). Influence of creep strains (which relax the induced stresses) will be studied on the predicted damage field and (eventual) associated reduction of material mechanical properties (Young modulus and tensile strength). It is worth noting that, in this contribution only the material mechanical properties modification linked to the material scale is studied and that for the analyses of a massive concrete structure the structural effect of restrained shrinkage must be taken into account.

## 2 HYDRATION MODELLING

### 2.1 Chemo-thermal model

The prediction of early-age behavior required to know the evolution of the concrete hydration. This evolution can be achieved by the use of a chemical affinity [17] and

considering that the reaction is thermo-activated following the Arrhenius law [18-19]:

$$\dot{\xi} = \tilde{A}(\xi) \exp\left(-\frac{E_a}{RT}\right) \quad (1)$$

where  $E_a$  is the activation energy,  $R$  is the ideal gas constant  $8.3145 \text{ J.K}^{-1}\text{mol}^{-1}$ ,  $T$  is the temperature,  $\xi$  is the hydration degree and  $\tilde{A}(\xi)$  is the chemical affinity.

To obtain the temperature evolution, the energy balance equation, which includes the heat release due to hydration reaction, is solved:

$$CT\dot{=} = \nabla(k\nabla T) + L\dot{\xi} \quad (2)$$

in which  $L$  is the latent hydration heat [ $\text{J.m}^{-3}$ ],  $k$  is the thermal conductivity [ $\text{W.m}^{-1}\text{K}^{-1}$ ] and  $C$  is the volumetric heat capacity [ $\text{J.m}^{-3}\text{K}^{-1}$ ], which are assumed constant [20-21].

The thermal boundary conditions are assumed to be of convective type. The convective heat flux  $\boldsymbol{\varphi}$  [ $\text{W.m}^{-2}$ ] reads:

$$\boldsymbol{\varphi} = h(T_s - T_{ext})\mathbf{n} \quad (3)$$

where  $h$  is the exchange coefficient including convection and radiation (after linearization) [ $\text{W.m}^{-2}\text{K}^{-1}$ ],  $T_s$  is the temperature on the surface [K] and  $T_{ext}$  is the ambient temperature [K].

### 2.2 Autogeneous and thermal strain model

Autogenous shrinkage  $\boldsymbol{\varepsilon}_{au}$  and thermal strain  $\boldsymbol{\varepsilon}_{th}$  can be modelled by the following equations:

$$\boldsymbol{\varepsilon}_{au} = -\kappa \bar{\xi} \mathbf{1} \quad \text{and} \quad \boldsymbol{\varepsilon}_{th} = \alpha(T - T_0) \mathbf{1} \quad (4)$$

$$\text{with} \quad \bar{\xi} = \left\langle \frac{\xi - \xi_0}{\xi_\infty - \xi_0} \right\rangle_+$$

where  $\kappa$  is a constant material parameter,  $\xi_0$  is the mechanical percolation threshold,  $\xi_\infty$  is the final hydration degree,  $\langle \cdot \rangle_+$  is the positive part

operator and  $\alpha$  is the coefficient of thermal expansion.

### 2.3 Cracking model

The mechanical behaviour of concrete is modelled by an isotropic elastic damage model coupled with creep. Such model reveals to be sufficient for predicting cracking due to restrained strain [16][13]. The Young modulus  $E$  and the tensile strength  $f_t$  increase due to hydration as follows [22-23]:

$$E(\xi) = E_\infty \bar{\xi}^{a_E} \quad \text{and} \quad f_t(\xi) = f_{t_\infty} \bar{\xi}^{a_{f_t}} \quad (5)$$

where  $E_\infty$  and  $f_{t_\infty}$  are the final Young modulus and tensile strength, respectively (i.e. when  $\xi = \xi_\infty$ ),  $a_E$  and  $a_{f_t}$  is a constant material parameters.

The evolution of the tensile strain threshold is then computed from the evolution of tensile strength and the Young modulus:

$$\kappa_0(\xi) = \frac{f_t(\xi)}{E(\xi)} = \frac{f_{t_\infty}}{E_\infty} \bar{\xi}^{\gamma-\beta} \quad (6)$$

The Poisson ratio is relatively stable for concrete. Neville [24] recommends a value equal to 0.2 for most concrete mixes. However, De Schutter and Taerwe [25] suggests an evolution depending on the hydration degree, which has been considered here:

$$\nu(\xi) = 0.18 \sin \frac{\pi \xi}{2} + 0.5 \exp(-10\xi) \quad (7)$$

where  $\nu$  is the Poisson ratio and  $\xi$  is the hydration degree.

The relationship between apparent stresses  $\boldsymbol{\sigma}$ , effective stresses  $\tilde{\boldsymbol{\sigma}}$ , damage  $D$ , elastic stiffness tensor  $\mathbf{E}$ , elastic strains  $\boldsymbol{\epsilon}_e$ , basic creep strains  $\boldsymbol{\epsilon}_{bc}$ , total strains  $\boldsymbol{\epsilon}$ , and previously defined strains reads:

$$\begin{aligned} \boldsymbol{\sigma} &= (1-D)\tilde{\boldsymbol{\sigma}} = (1-D)\mathbf{E}(\xi)\dot{\boldsymbol{\epsilon}}_e \\ &= (1-D)\mathbf{E}(\xi)(\dot{\boldsymbol{\epsilon}} - \dot{\boldsymbol{\epsilon}}_{bc} - \dot{\boldsymbol{\epsilon}}_{au} - \dot{\boldsymbol{\epsilon}}_{th}) \end{aligned} \quad (8)$$

$D$  is linked to the elastic equivalent tensile strain ( $\hat{\epsilon}$ ) and the damage criterion is given by Mazars [26]:

$$f = \hat{\epsilon} - \kappa_0(\xi) \quad (9)$$

where  $\kappa_0(\xi)$  is the tensile strain threshold.

Then,  $\dot{D} = 0$  if  $\hat{\epsilon} \leq \kappa_0(\xi)$  and if  $\hat{\epsilon} \geq \kappa_0(\xi)$ :

$$D = 1 - \frac{\kappa_0}{\hat{\epsilon}} \left[ (1 + A_t) \exp(-B_t \hat{\epsilon}) - A_t \exp(-2B_t \hat{\epsilon}) \right] \quad (10)$$

where  $A_t$  and  $B_t$  are constant material parameters which control the softening branch in the stress-strain curve in tension.

High stress levels lead to non-linear creep strains (which may induce failure). Following Mazzotti and Savoia [27-30], a part (controlled by parameter  $\beta$ ) of creep strains  $\boldsymbol{\epsilon}_{bc}$  (see paragraph 2.4) is included into the expression of the equivalent strain defined by Mazars [26][31]:

$$\hat{\epsilon} = \sqrt{\langle \boldsymbol{\epsilon}_e + \beta \boldsymbol{\epsilon}_{bc} \rangle_+ : \langle \boldsymbol{\epsilon}_e + \beta \boldsymbol{\epsilon}_{bc} \rangle_+} \quad (11)$$

Strain softening induces inherent mesh dependency and produces failure without energy dissipation [32]. In order to dissipate the same amount of energy after mesh refinement, when strains localise in one row of finite elements, a characteristic length  $l_c$  is introduced which is related to the mesh size [33-34].

For the adopted model, the dissipated energy density  $g_{ft}$  at failure in tension reads:

$$g_{ft}(\xi) = \frac{f_t(\xi)(1 + A_t/2)}{B_t} \quad (12)$$

It is related to the fracture energy  $G_{ft}$  and the characteristic length  $l_c$ :

$$g_{ft}(\xi) = \frac{G_{ft}(\xi)}{l_c} \quad (13)$$

$$l_c = \sqrt[3]{V_{ef}}$$

where  $V_{ef}$  is the volume of the finite element. The fracture energy also depends on the hydration degree [35]:

$$G_{f_i}(\xi) = G_{f_{i\infty}} \bar{\xi}^\delta \quad (14)$$

For a CEM I 52.5, De Schutter and Taerwe [35] found that  $\delta=0.46$  fits well experimental data. This value has been used for the finite element simulations.

## 2.4 Creep model

The model takes into account directly effects of hydration. In order to reproduce the (partial) reversible part of basic creep, Kelvin-Voigt and dashpot chains are used. The strains can be obtained by solving the following differential equations [36]:

$$\tau_{bc}^i \ddot{\epsilon}_{bc}^i + \left( \tau_{bc}^i \frac{k_{bc}^i(\xi)}{k_{bc}^i(\xi)} + 1 \right) \dot{\epsilon}_{bc}^i = \frac{\dot{\sigma}}{k_{bc}^i(\xi)} \quad \text{and} \quad (15)$$

$$\dot{\sigma} = \eta_{bc}^i(\xi) \dot{\epsilon}_{bc}^j$$

where  $\tau_{bc}^i$  is the characteristic time (constant),  $k_{bc}^i(\xi)$  and  $\eta_{bc}^j(\xi)$  are the spring stiffness and viscosity, respectively (increasing with the hydration degree) and  $\dot{\sigma}$  is the previously defined effective stress (equation 8).

The stiffness parameter for each unit is calculated with the following equation proposed by de Schutter [22] and slightly modified [36]:

$$k_{bc}^i(\xi) = k_{bc-\infty}^i \frac{0.473}{2.081 - 1.608 \bar{\xi}} \bar{\xi}^\psi \quad (16)$$

$$\text{and } \eta_{bc}^j(\xi) = \eta_{bc-\infty}^j \frac{0.473}{2.081 - 1.608 \bar{\xi}} \bar{\xi}^\psi$$

where  $k_{bc-\infty}^i$  and  $\eta_{bc-\infty}^j$  are the final stiffness and viscosity, respectively. The characteristic time ( $\tau = k_{bc}^i(\xi)/\eta_{bc}^j(\xi)$ ) is assumed to be constant for the Kelvin-Voigt unit.

At this time, tensile creep is considered to have the same amplitude and kinetic that compressive one, due to the lack of relevant data (especially for cement pastes, where there is no data to the authors' knowledge). Besides, the previous equations are extended into multiaxial stress state using a creep Poisson ratio, taken equal to the elastic one.

## 2.5 Mesoscopic mesh

The algorithm of mesh generation was developed by Nguyen *et al.* [37].

Numerical simulations are performed on a 2D REV of concrete of  $100 \times 100 \text{ mm}^2$  (see Figure 1), where the cement paste and the aggregate are meshed (the calculations are performed in the context of plane stresses) using an original technique [37]: both phases are not explicitly meshed, instead material properties are projected on a existing fine mesh. The mesostructure is representative in term of aggregate content and sizes distribution of an ordinary concrete that has been deeply investigated experimentally [38] [13] [5]. As the ITZ is not considered, a perfect bond could be assumed between cement paste and aggregates.

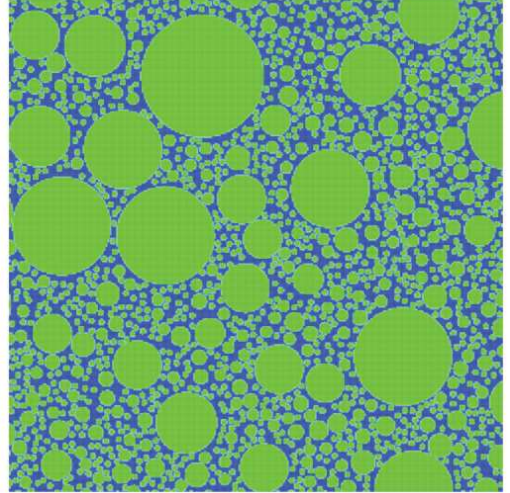


Figure 1: Mesh of the REV.

## 2.6 Boundary conditions and material parameters

The algorithm of mesh generation was developed by Nguyen *et al.* [37]. A massive concrete wall of 1.2 m thick is considered. One area is extracted (in the core) and is applied in a uniform way to the REV of concrete, using adapted mechanical boundary conditions (Figure 2):

The displacement of all the sides are partially restrained.

The partial restraint consists of constraining the same uniform displacement in the concerning sides through adapted kinematic relations. Additional kinematic relations are

used to eliminate rigid body displacements. It is worth noting that the used boundary conditions are not exactly representative of real boundary conditions.

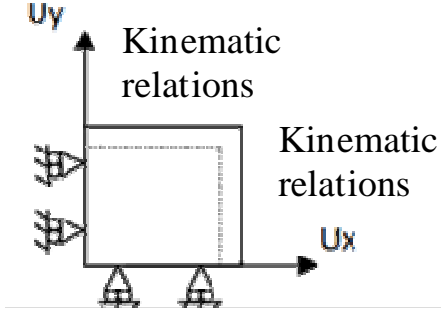


**Figure 2:** Mechanical boundary conditions

An ordinary concrete is considered. Using experimental data [13] and numerical analysis [13][36], temperature field evolution is predicted (figure 3). In the thermal simulation the heat exchange coefficient ( $h$ ) is adjusted to reproduce experimental temperature evolution of a massive wall of ordinary concrete [39]. Creep parameters and autogenous shrinkage amplitude of the cement paste are also adjusted to reproduce, with a mesoscopic simulation (only the cement paste is undergoing creep and shrinkage), the results obtained on an ordinary concrete by experimental test [40]. The table 1 gives the value of used parameters for cement paste and aggregates.

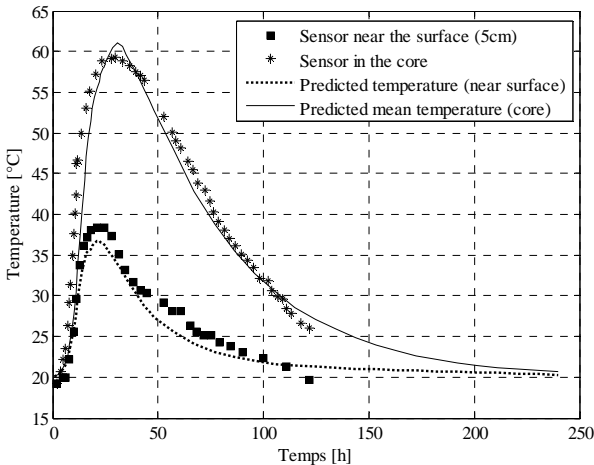


**Figure 3:** Comparison between experimental temperature for an ordinary concrete and numerical temperature taken into account.

**Table 1:** Parameters of cement paste used in the mesoscopic simulations

Parameter		OC cement paste	Aggregates
Total heat released	L	6.06e8 J/m <sup>3</sup>	-
Creep parameters	$k_{bc-\infty}^1$ ( $\tau=0.1$ days)	7.5e10 Pa	-
	$k_{bc-\infty}^2$ ( $\tau=1$ days)	2.25e10 Pa	-
	$k_{bc-\infty}^3$ ( $\tau=10$ days)	6.25e9 Pa	-
Young modulus	E	15 GPa	60GPa
Tensile strength	$f_t$	1,5 MPa	-
Shrinkage amplitude	$\kappa$	160 $\mu\text{m}/\text{m}$	-
Thermal dilatation coefficient	$\alpha$	15 $\mu\text{m}/(\text{m}\cdot^\circ\text{C})$	5 $\mu\text{m}/(\text{m}\cdot^\circ\text{C})$

To highlight the modification of the concrete behaviour due to the mesoscopic representation and due to hydration, homogeneous simulations of the same specimen have also been performed.

The elastic mechanical parameters of the homogeneous simulation have been calculated from the parameters of cement paste and aggregates by using the Mori-Tanaka approach [41].

### 3 STRESSES AND DAMAGE FIELDS AFTER HYDRATION

Numerical simulations are performed on the concrete REV to compute the evolution of damage field at early-age due to incompatibilities of strain (autogenous shrinkage and slight mismatch of coefficient of thermal expansion) between cement paste and aggregates. Influence of creep is studied. Damage fields at different times are displayed on Figure 4. The cracking probability is the results of a competition between generated stresses induced by differential shrinkage (thermal and autogenous one), creep strains, Young modulus and the tensile strength evolutions.

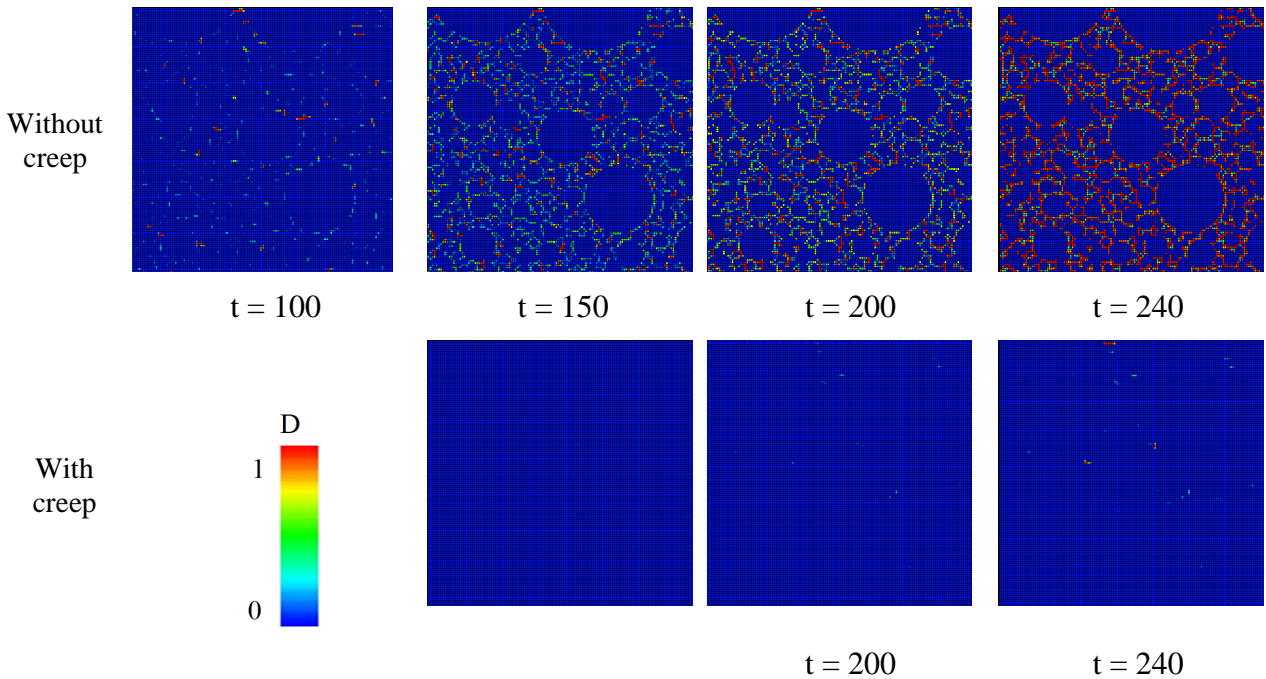


**Figure 4:** Evolution of the damage field (D) during hydration for OC: Influence of the creep (t represent the time (in hours) after casting)

The numerical results show that, since the creep in the cement paste of an ordinary concrete is very large (compared to concrete or a high performance cement paste), a very important relaxation of stresses occur and decreases the micro-cracking density. Therefore, damage due to strain incompatibilities at early-age are largely overestimated and may lead to a (misleading) significant decrease of mechanical properties if creep is not taken into account. On the opposite and as expected, creep tends to limit (and localize) damage areas, since autogeneous shrinkage is very limited for an

ordinary cement paste and since the mismatch of thermal expansion due to the variation of temperature induced by hydration is limited. In this case, the influence of internal stresses developed at early-age need to be studied. Figure 5 and 6 shows the internal stress field obtained after hydration. The residual internal stresses are more important when creep is taken into account because without creep, cracking occurs which reduces the apparent stresses.

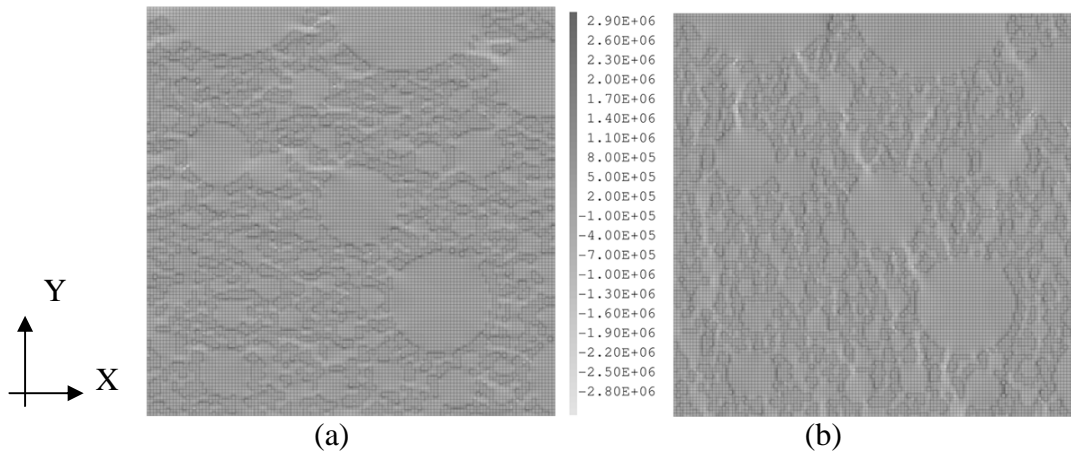


**Figure 5:** Initial stresses after hydration for simulation at the core without taking into account creep for ordinary concrete:  $\sigma_{XX}$  (a),  $\sigma_{YY}$  (b)

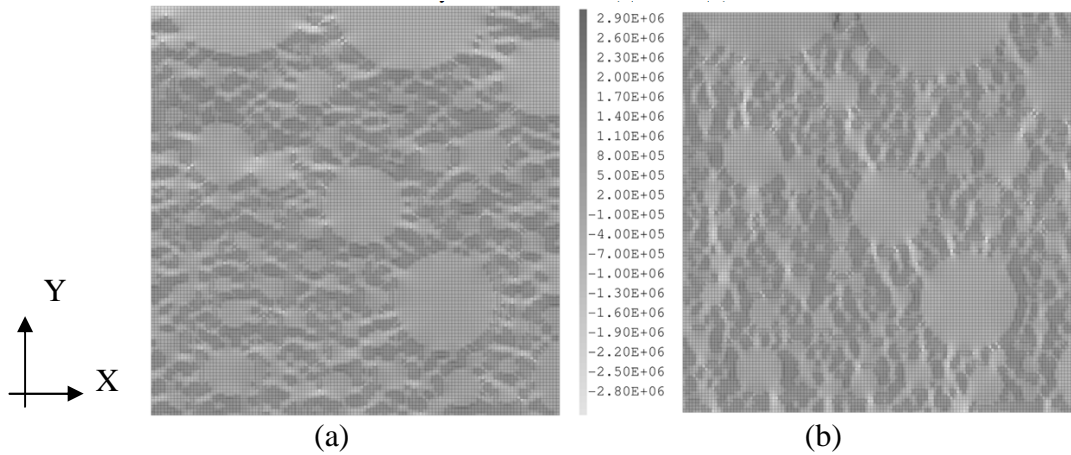


**Figure 6:** Initial stresses after hydration for simulation at the core with taking into account creep for ordinary concrete:  $\sigma_{XX}$  (a),  $\sigma_{YY}$  (b)

#### 4 GLOBAL BEHAVIOUR AFTER HYDRATION

After the initial computation of internal strains and stresses in the REV concrete (see previous part), the global behaviour of the concrete is computed by a simulation of a cyclic loading (tensile uniaxial stresses followed by compressive ones). As irreversible strains are not considered in the used damage model, the crack closure stress should be equal to  $\sigma_c=0\text{MPa}$ . In the case of cyclic loading, during the load reversal, micro-cracks close progressively and the tangent stiffness of the material should then increase. The damage model proposed in the paragraph 2 is not able to reproduce this stiffness increasing. So, for the following simulations, the unilateral effect is taken into account by a separation of the stress tensor into positive and negative parts [14]. The stress is given by:

$$\sigma = (1 - D)\tilde{\sigma}_+ + (1 - D)^\alpha \tilde{\sigma}_- \quad (17)$$

Where  $\sigma_+$  and  $\sigma_-$  are the positive and the negative part of the stress tensor,  $\alpha$  is a constant parameter and  $D$  is the damage variable.

Figure 6 displays the stress – strain relationship (which could be called behavior law) of ordinary concrete during the test for four situations:

- 1 OC - Homoref : Homogeneous and same parameters for cement paste and aggregates without hydration (the mesoscopic nature of concrete is not considered)
- 2 OC - Mesoref : different parameters are considered for cement paste and aggregates without hydration (the mesoscopic nature of concrete is considered)
- 3 OC - Meso hydration with creep core : different parameters are considered for cement paste and aggregates (the mesoscopic nature of concrete is considered), initial stresses, damage state due to hydration and creep are taken into account
- 4 OC - Meso hydration core: different parameters are considered for cement paste and aggregates (the mesoscopic nature of concrete is considered), initial stresses and damage state due to hydration are taken into account but creep is neglected

The difference between the case 1 and 2 is only due to the mesoscopic representation of the concrete. One can remark that an important decrease on the maximal strength is obtained du to a more gradual cracking process but also that the value of the crack closure stress is modified. When hydration is taken into account and induces initial stresses and

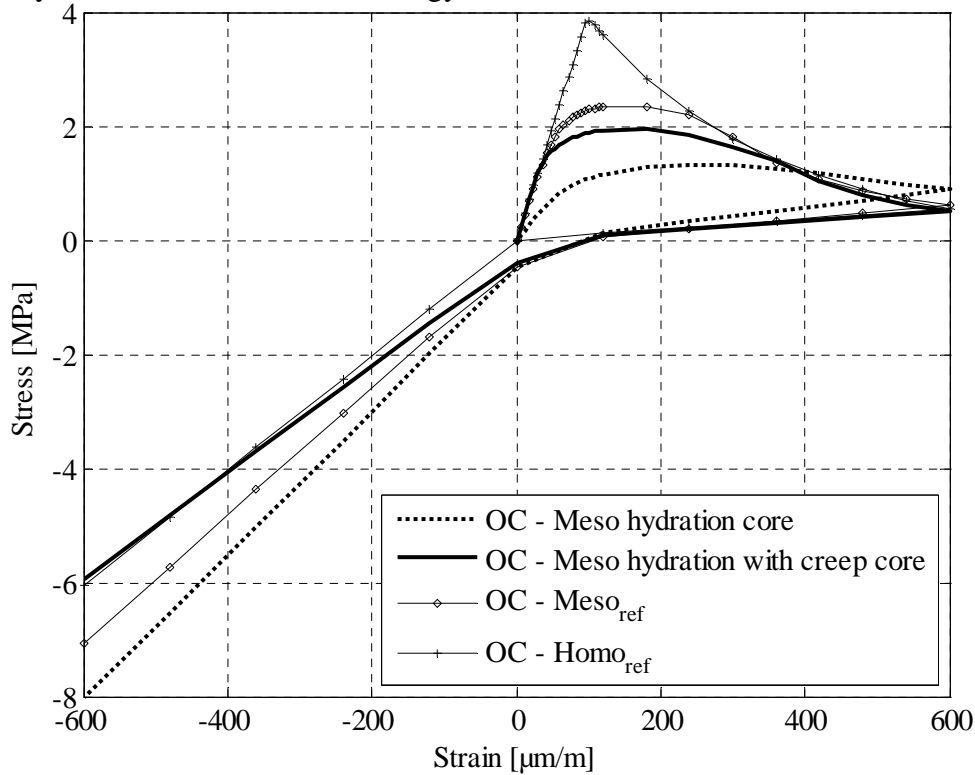
damage, a significant decrease of the stiffness and of the maximal stress is predicted if creep is not taken into account (about 50%) whereas when creep is taken into account, initial stresses are relaxed and only few elements are affected by initial damage. Thus, only a slight decrease of the maximal reached stress is obtained (about 18%). This last case is considered as the closer to the realistic one and will be considered as the reference case for the following comparisons.

It is interesting to note that when an important initial damage field is obtained after hydration (case OC- hydration when creep is not taken into account), the global behavior seems to be more ductile. The same results were obtained by Heinfling et al. [42]. This could be explained by more distributed energy

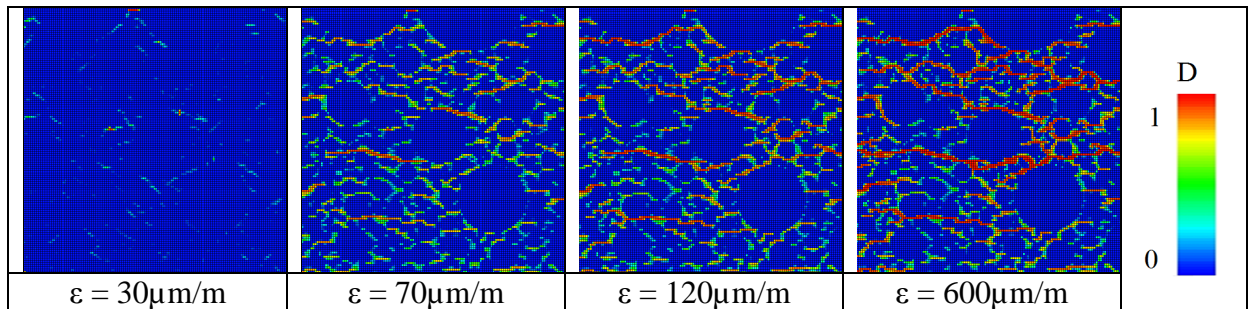
dissipation. Indeed, figure 8 shows the damage field evolution during tensile test and one can see that damage areas are more important during tensile test when creep is not taken into account during hydration calculation (increase of 22% of the equivalent number of elements where the damage is equal to 1 defined as

$$n_{eq}(D=1) = \frac{\int_S D dS}{\int_s ds}$$

where S is the surface of the mesoscopic mesh and s is the surface of one element).



**Figure 7:** Global behavior during the tensile – compression loading cycle for OC at the wall core



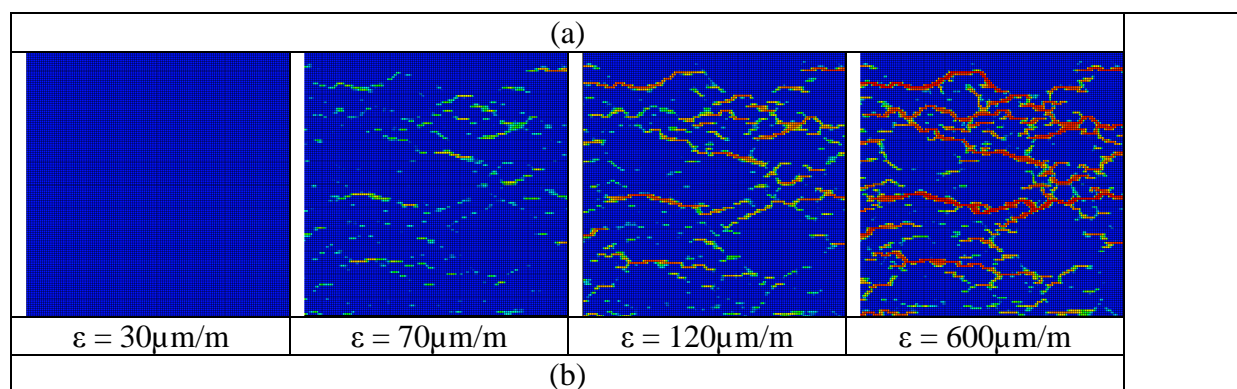


**Figure 8:** Evolution of the damage field (D) during hydration for OC when creep is taken into account (a) or not (b)  $\varepsilon$  is the global imposed strain during tensile test

## 5 CONCLUSION

A numerical chemo-thermo-mechanical procedure applied on a concrete mesostructure has been used to calculate the initial stresses and damage state due to hydration on a massive wall for OC with taking into account explicitly aggregate and cement paste. Autogenous shrinkage and different thermal dilatation coefficient between cement paste and aggregate have been considered. The impacts of the initial state on the uniaxial tensile behaviour and unilateral effect have been discussed. Regarding the cyclic behavior, these initial states seem to play an important role. Indeed, it is shown on an ordinary concrete that autogenous and thermal shrinkage lead to small uniform micro-cracking when creep is taken into account but the initial stress state modify the global behavior. It induces a slight reduction of apparent elastic stiffness and tensile strength. Moreover, the mesoscopic mesh and the mechanical properties gradient between cement paste and aggregates lead to the obtaining of a crack closure stress ( $\sigma_c < 0$ MPa) even if plastic strains are not included in the model. Therefore, a multi-scaled coupled approach should be used and the next step of this study will be to associate the mesoscopic structure in a massive wall simulation (using relation between displacement or/and nodal forces at the interfaces of both domains).

## REFERENCES

- [1] Hobbs DW. (1974) Influence of aggregate restraint on the shrinkage of concrete, *ACI J*, Vol.71, pp.445–50.
- [2] Bisschop J. and Van Mier J.G.M. (2002) Effect of aggregates on drying shrinkage microcracking in cement-based composites. *Mater Struct*, Vol. 35, pp. 453–61.
- [3] Hubert F-X, Burlion N and Shao J.F. (2003) Drying of concrete: modelling of a hydric damage. *Mater Struct*, Vol.36, pp.12–21.
- [4] Grassl P, Wong H.S. and Buenfeld N.R. (2010), Influence of aggregate size and volume fraction on shrinkage induced micro-cracking of concrete and mortar. *Cem Concr Res*, Vol. 40, pp. 85–93.
- [5] Lagier F., Jourdain X., De Sa C., Benboudjema F. and Colliat J.B. (2011), Numerical strategies for prediction of drying cracks in heterogeneous materials: comparison upon experimental results, *Engineering Structures*, Vol. 33(3), pp. 920 – 931.
- [6] Idiart A., Bisschop J., Caballero A. and Lura P., (2012), A numerical and experimental study of aggregate-induced shrinkage cracking in cementitious composites, *Cement and Concrete Research*, Vol.42, pp. 272–281

- [7] Xotta G., Salomoni V.A. and Willam K.J.(2011), Macro vs. Meso-scale Modelling of Concrete under High Temperature Conditions, International Conference on Computational Modeling of Fracture and Failure of Materials and Structures, 6-8 June 2011 Barcelona, Spain
- [8] Grondin F., Dumontet H., Ben Hamida A. and Boussa H. (2011), Micromechanical contributions to the behaviour of cement-based materials: Two-scale modelling of cement paste and concrete in tension at high temperatures, *Cement and Concrete Composites*, Vol.33(3), pp. 424–435
- [9] Grassl P. and Pearce C. (2010), Mesoscale Approach to Modeling Concrete Subjected to Thermomechanical Loading, *Journal of Engineering Mechanics*, Vol. 136(3), pp. 322-328,
- [10] de Sa C. and Benboudjema F., (2008) Separation of damage mechanisms in concrete at high temperature, contribution of a mesoscopic approach. *GeoProc 2008 - 3rd International Conference on Coupled T-H-M-C processes in Geo-Systems*. 2008.
- [11] Schlangen E., Leegwater G. and Koenders E.A.B. (2006), Modelling of autogenous shrinkage of concrete based on paste measurements, 2nd International Symposium on Advances in Concrete through Science and Engineering 11-13 September 2006, Quebec City, Canada
- [12] Garboczi, E. J. and Bentz, D. P. (1997), Analytical formulas for interfacial transition zone properties, *Adv. Cem. Bas. Mat.*, Vol. 6, pp.99–108
- [13] Briffaut, M., Benboudjema, F., Torrenti, J.-M. and Nahas, G. (2011), Numerical analysis of the thermal active restrained shrinkage ring test to study the early age behavior of massive concrete structures, *Engineering Structures*, vol. 33(4) pp.1390-1401.
- [14] Fichant S. La Borderie C. and Pijaudiet-Cabot G. (1999), Isotropic and anisotropic description of damage in concrete structures, *Mech. Cohes.-Frict Mater.*, Vol. 4, pp. 339-359.
- [15] Matallah M, La Borderie C. and Maurel O. (2010), A practical method to estimate crack openings in concrete structures. *Int J Numer Anal Methods Geomech*, Vol.34(15), pp.1615–33.
- [16] De Sa C., Benboudjema F., Thiery M. and Sicard J. (2008), Analysis of microcracking induced by differential drying shrinkage, *Cement and Concrete Composites*, Vol.30(10), pp. 947-956.
- [17] Ulm, F.-J. and Coussy, O. (1998), ‘Couplings in early-age concrete: from material modelling to structural design’, *International Journal of Solids and Structures* Vol. 35(31-32) pp. 4295-4311.
- [18] Lackner R., Mang H.A., Chemoplastic material model for the simulation of early-age cracking: From the constitutive law to numerical analyses of massive concrete structures, *Cement & Concrete Composites*, pp. 551–562, Vol. 26, 2004.
- [19] Regourd M., Gauthier E., Behavior of cement under accelerated hardening, *Annales de l’ITBTP* 179 (in French), 1980, pp. 65-96, 1980.
- [20] Waller V., d’Aloia L., Cussigh F. and Lecrux S. (2004), Using the maturity method in concrete cracking control at early ages, *Cement & Concrete Composites*, Vol. 26, pp. 589–599.
- [21] Briffaut, M., Benboudjema, F., Torrenti, J.-M. and Nahas, G. (2012a), Effects of early-age thermal behaviour on damage risks in massive concrete structures, *European Journal of Environmental and Civil Engineering*, Vol. 16(5), pp. 589–605
- [22] De Schutter, G. (1999), Degree of hydration based Kelvin model for the basic creep of early age concrete, *Materials and Structures*, Vol.32 pp260-265.

- [23] Stefan L., Benboudjema F., Torrenti J.M., Bissonnette B., Prediction of elastic properties of cement pastes at early ages, *Computational Materials Science*, pp. 775-784, Vol. 47, 2010.
- [24] Neville A.M., Dilger W.H. and Brooks J.J. (1983), creep of plain and structural concrete, Longman group construction press.
- [25] De Schutter G. and Taerwe L. (1996), Degree of hydration-based description of mechanical properties of early age concrete, *Materials and Structures*, Vol. 29, pp. 335–44.
- [26] Mazars J. (1986), A description of micro and macroscale damage of concrete structures, *Engineering Fracture Mechanics*, Vol. 25, pp. 729-737.
- [27] Mazzotti C., Savoia M. (2003), Nonlinear Creep Damage Model for Concrete under Uniaxial Compression. *Journal of Engineering Mechanics*, vol.129(9), p.1065-1075.
- [28] Omar M., Loukili A., Pijaudier-Cabot G. and Le Pape Y. (2009), Creep damage coupled effects : experimental investigations on bending beams of different sizes, *Advanced Engineering Materials*, Vol. 21, pp. 65-72
- [29] Reviron N., Benboudjema F., Torrenti J.M., Nahas G. and Millard A. (2007), A Coupling between creep and cracking in tension. *FraMCoS 6 - 6th International Conference on Fracture Mechanics of Concrete and Concrete Structures*, 2007.
- [30] de Larrard T., Benboudjema F., Colliat J.-B., Torrenti J.-M. and Deleruyelle F. (2010), Uncertainty propagation on damage evolution of a concrete structure submitted to coupled leaching and creep, *European Journal of Environmental and Civil Engineering*, Vol 14(6/7), pp. 891-921
- [31] Torrenti, J. M., Nguyen, V. H., Colina, H., Le Maou, F., Benboudjema, F. and Deleruyelle, F. (2008), Coupling between leaching and creep of concrete, *Cement and Concrete Research*, vol. 38(6), pp. 816-821.
- [32] Pijaudier-Cabot G. and Bažant Z.P. (1987), Nonlocal damage theory, *J. of Engrg. Mech. ASCE*, Vol. 113, pp. 1512-1533.
- [33] Rots J.G. (1988), Computational modeling of concrete fracture, Netherlands: Delft University of Technology PhD Dissertation.
- [34] Cervera M. and Chiumenti M. (2006), Mesh objective tensile cracking via a local continuum damage model and a crack tracking technique, *Computat. Methods Appl. Mech. Engrg*, Vol. 196, pp. 304-320.
- [35] De Schutter G. and Taerwe L. (1997), Fracture energy of concrete at early ages, *Materials and structures*, Vol. 30, pp. 67-71.
- [36] Benboudjema, F. and Torrenti, J.-M. (2008), Early-age behaviour of concrete nuclear containments, *Nuclear, Engineering and Design*, Vol. 238, pp. 2495-2506.
- [37] Nguyen T.D., Lawrence C., La Borderie C., Matallah M. and Nahas G. (2010), A mesoscopic model for a better understanding of the transition from diffuse damage to localized damage, *European Journal of Environment and Civil Engineering*, Vol.14(6-7), pp.751-776.
- [38] Reviron N. (2009), Study of creep of concrete in tension. Application to the nuclear pressurized water containment, PhD thesis ENS Cachan, LMT, in French.
- [39] Ithurrealde G. (1989), La perméabilité vue par le maître d’ouvrage, *Ecole Normale Supérieure. Cachan : Colloque Béton à hautes performances*.
- [40] Briffaut, M., Benboudjema, F., Torrenti, J.-M. and Nahas, G. (2012b), Concrete early age basic creep : experiments and test of rheological modelling approaches,

accepted in Construction and buildings materials.

- [41]Mori, T. and Tanaka, K. (1973), Average stress in matrix and average elastic energy of materials with misfitting inclusions , Acta Metallurgica, Vol. 21, pp. 571-574.
- [42]Heinfling G, Stabler J., Baker G. and Reynouard J.M. (1998), Effects of high temperatures on the fracture energy of concrete, International Conference on Fracture Mechanics of Concrete Structures, FRAMCOS 3 (3rd), 1998